Resistivity and Hall effect of EuSe in fields up to 150 kOe

Y. Shapira, S. Foner, and N. F. Oliveira, Jr.*

Francis Bitter National Magnet Laboratory,† Massachusetts Institute of Technology, Cambridge, Massachusetts 02139

T. B. Reed‡

Lincoln Laboratory, Massachusetts Institute of Technology, Lexington, Massachusetts 02173

The resistivity $\rho(H_{ext}, T)$ and Hall effect were studied in ten n-type EuSe single-crystal samples with room-temperature carrier concentrations from 4.2×10^{18} to 3.5×10^{19} electrons/cm^3. The electrical measurements were performed at temperatures $1.6 \leq T \leq 300$ K and external magnetic fields $0 \leq H_{ext} \leq 150$ kOe, and were supplemented by magnetization and differential susceptibility measurements to aid in the interpretation. The following phenomena were observed: (a) A very large peak in the zero-field resistivity occurred at a temperature T_{max} which varied from ~ 7 to ~ 13 K, depending on the sample. (b) A negative magnetoresistance was observed for most temperatures and was very large near T_{max}. (c) However, in a limited temperature interval well above T_{max}, a positive magnetoresistance was observed at low fields (followed by a negative magnetoresistance at higher fields). (d) Below ~ 3 K, the zero-field resistivity increased rapidly with decreasing T, except for the sample with the highest carrier concentration. (e) The anomalous Hall effect was negligible at temperatures $T \lesssim 4.2$ K. Much of the data are interpreted in terms of band conduction. The mobility is then limited by spin-disorder scattering and it increases with increasing H_{ext}, resulting in a negative magnetoresistance. This description fails when both $T \lesssim T_{max}$ and $H_{ext} < 1$ to 10 kOe. Under these conditions, the very high resistivity is attributed to the localization (trapping) of electrons by the s-f (or d-f) interaction. At temperatures for which the electrons are localized at $H_{ext} = 0$, a field of 1 to 10 kOe delocalizes the electrons and, therefore, leads to band conduction and a much lower resistivity. At higher fields there is a negative magnetoresistance (smaller than at low fields) due to the reduction in spin-disorder scattering of the band electrons. A model for the positive magnetoresistance, which focuses on the spin splitting of the conduction band by a magnetic field, is presented in the following paper.

I. INTRODUCTION

The Eu chalcogenides (EuO, EuS, EuSe, and EuTe) are semiconductors which order magnetically at low temperatures. When samples of these materials contain donors, conduction electrons and/or localized electrons are present. Much of the interest in the Eu chalcogenides centers on those properties which arise from the strong s-f (or d-f) interaction between the spins of the Eu^{++} ions on one hand, and the spins of conduction or localized electrons on the other. This interaction leads to a very strong dependence of the electrical-transport and optical properties on the magnetic order of the Eu^{++} spins. In addition, the presence of conduction or localized electrons leads to an indirect coupling between the Eu^{++} spins, which results in changes of the magnetic properties such as the Curie-Weiss temperature Θ. These effects have been reviewed by Methfessel and Mattis,[1] and by Haas.[2]

The Eu chalcogenides have the NaCl structure, in which the Eu^{++} ions form a fcc lattice. Each Eu^{++} ion has seven electrons in a half-filled $4f$ shell, giving rise to a magnetic moment of $7\mu_B$ per ion, where μ_B is the Bohr magneton. The magnetic order in pure Eu chalcogenides (i.e., in the absence of impurities, nonstoichiometry, or crystal defects) is

believed to be determined primarily by a competition between a ferromagnetic nearest-neighbor exchange interaction and an antiferromagnetic next-nearest-neighbor exchange interaction (Ref. 1, p. 507 ff). The ferromagnetic interaction dominates in EuO (Curie temperature $T_C = 69$ K) and in EuS ($T_C = 16$ K), but not in EuTe which is antiferromagnetic (Néel temperature $T_N = 9.6$ K). In EuSe the ferromagnetic and antiferromagnetic interactions are comparable, resulting in several magnetic phases with different magnetic order. This complexity is reflected in the electrical transport properties of EuSe. The magnetic phase diagram of EuSe is discussed in Sec. III.

In the present paper we describe the results of electrical-resistivity and Hall-effect measurements on n-type EuSe single crystals, in magnetic fields up to 150 kOe. This work follows our high-magnetic-field studies of electrical transport in EuO,[3,4] EuS,[4,5] and EuTe.[6] Earlier studies of the resistivity of Gd-doped EuSe were reported by Holtzberg et al.,[7] Methfessel,[8] and von Molnar and Methfessel.[9] Among these, von Molnar and Methfessel gave the most extensive account of the temperature and magnetic-field dependence of the resistivity, and presented results of Hall measurements. The most prominent features of their data were a large resis-

tivity peak near the magnetic-ordering temperature, and a large negative magnetoresistance which was studied in fields up to 14 kOe. The use of magnetic fields up to 150 kOe in the present work has made it possible to obtain more complete data than those reported earlier, and to uncover new phenomena such as the positive magnetoresistance in a limited temperature range. Our data at zero and low magnetic fields are qualitatively similar to those in Ref. 9.

The early resistivity and Hall data for Gd-doped EuSe (Refs. 7–9) have been discussed extensively in the literature.[1,2,10-15] Some of the models in these discussions will be considered later when we interpret our data. In addition, a new model for the positive magnetoresistance will be presented in the following paper.[16]

II. EXPERIMENTAL TECHNIQUES

A. Samples

Electrical measurements were made on ten n-type EuSe samples, obtained by cleaving four single crystals. Different samples from the same single crystal will be labeled by the same number followed by different letters, e.g., 1A, 1B, 1C. The four crystals were grown from Eu-rich solutions of Eu

and Se using procedures described earlier.[17] Although the crystals were not intentionally doped, emission spectroscopic analyses on samples cut from crystals Nos. 1 and 3 showed the presence of small amounts of impurities. The concentrations of the principal impurities in crystal No. 1, in ppm, were Ca, 1 to 10; Mg, 1 to 10; Si, 1 to 10. The concentration of the principal impurities for sample No. 3 were: Mn, 10 to 100, Ca, 1 to 10; Cu, 1 to 10; Fe, 1 to 10, Mg, 1 to 10; Si, 1 to 10; Yb, 1 to 10. Additional inert-gas fusion analysis for oxygen in crystal No. 1 gave a concentration of 0.036 wt %. We presume that the conduction electrons in our samples were mainly due to the excess Eu.

All samples were rectangular parallelepipeds, with faces parallel to the {100} planes and with typical dimensions of $1 \times 1 \times 4$ mm. Some of the electrical properties of the samples are listed in Table I. Hall measurements at room temperature showed that the concentration of conduction electrons varied from sample to sample between 4.2×10^{18} and 3.5×10^{19} cm^{-3}. Magnetization and differential susceptibility measurements were performed on several of the ten samples, and also on an additional nonconducting sample obtained from Professor G. E. Everett. The room-temperature resistivity of the nonconducting sample was $\rho(297 \text{ K}) \gtrsim 10^7$ Ωcm.

TABLE I. Electrical properties of the EuSe samples.[a]

Sample No.	1A	1B	1C	2A	2B	2C	2D	2E	3	4
$\rho(0, 297$ K) (Ω cm)	2.56×10^{-2}	4.6×10^{-2}	4.0×10^{-2}	2.9×10^{-2}	...	...	1.0×10^{-2}	1.52×10^{-2}	2.0×10^{-2}	3.5×10^{-3}
$R(100$ kOe, 297 K) (cm^3/C)	-0.80	-1.1	-1.48	-0.565	-0.6	...	-0.40	...	-0.51	-0.178
$n(100$ kOe, 297 K) (electrons/cm^3)	7.8×10^{18}	5.5×10^{18}	4.2×10^{18}	1.10×10^{19}	1.0×10^{19}	...	1.56×10^{19}	...	1.23×10^{19}	3.5×10^{19}
$\mu(100$ kOe, 297 K) (cm^2/V sec)	32	25	38	20	...	...	41	...	26	51
$\rho(0, 77.7$ K) (Ω cm)	3.02×10^{-2}	6.6×10^{-2}	5.8×10^{-2}	2.8×10^{-2}	...	...	...	1.35×10^{-2}	1.9×10^{-2}	2.43×10^{-3}
$\rho(100$ kOe, 77.7 K) (Ω cm)	2.42×10^{-2}	5.1×10^{-2}	4.4×10^{-2}	2.4×10^{-2}	...	...	...	...	1.7×10^{-2}	2.31×10^{-3}
$n(100$ kOe, 77.7 K) (electrons/cm^3)	8.9×10^{18}	5.6×10^{18}	...	1.15×10^{19}	1.1×10^{19}	...	...	...	1.25×10^{19}	3.55×10^{19}
$\mu(100$ kOe, 77.7 K) (cm^2/V sec)	29	22	...	22	...	...	...	...	29	76
$\rho(0, 4.2$ K) (Ω cm)	4.0×10^5	$\gtrsim 10^7$	1.2×10^7	22	~ 30	...	...	31	23	2.69×10^{-3}
$\rho(100$ kOe, 4.2 K) (Ω cm)	1.51×10^{-2}	2.6×10^{-2}	3.0×10^{-2}	1.55×10^{-2}	$\sim 1 \times 10^{-2}$	...	...	6.7×10^{-3}	1.1×10^{-2}	1.40×10^{-3}
$n(100$ kOe, 4.2 K) (electrons/cm^3)	8.9×10^{18}	...	...	1.2×10^{19}	1.1×10^{19}	8.8×10^{18}	...	...	1.30×10^{19}	3.69×10^{19}
$\mu(100$ kOe, 4.2 K) (cm^2/V sec)	46	...	...	35	...	...	...	...	44	121
T_{max} (K)	$5.9 < T < 7.8$	...	...	7.7 ± 0.2	...	...	...	7.5 ± 1	7.9 ± 0.2	13.4 ± 0.3
ρ_{max} (Ω cm)	$> 10^7$	...	...	3.5×10^5	...	...	...	...	5×10^4	3.7×10^{-2}

[a]$\rho(H_{ext}, T)$, $R(H_{ext}, T)$, $n(H_{ext}, T)$, and $\mu(H_{ext}, T)$ are, respectively, the resistivity, Hall coefficient, carrier concentration $1/R_0 e$, and Hall mobility, at an external magnetic field H_{ext} and temperature T. T_{max} is the temperature where the zero-field resistivity $\rho(0, T)$ has a maximum $\rho_{max} \equiv \rho(0, T_{max})$. For experimental uncertainties see text.

B. Electrical and magnetic measurements

Measurements of the dc electrical resistivity ρ and Hall voltage at temperatures $1.6 \leq T \leq 300$ K were performed using techniques similar to those used earlier.[3,5,6] Two improvements were the use of a Keithley 640 vibrating capacitor electrometer for measurements of high resistances, and the introduction of signal averaging equipment to improve the signal/noise ratio for the Hall measurements. The first improvement allowed measurements of resistances up to $\sim 10^8$ Ω, corresponding to $\rho \sim 10^7$ Ω cm (higher ρ could not be measured reliably because the resistance of the electrical insulation in the sample holder was between 10^9 and 10^{10} Ω). The signal-averaging equipment consisted of a voltage-to-frequency converter followed by a variable-time-base counter. Several successive ten sec readings of the counter were taken for each point, and the mean and standard deviation were obtained by a Wang 600 programmable calculator operating on line.

Resistivities were measured with an absolute accuracy of 20–50% depending on the particular sample. The uncertainty in each case reflected the uncertainty in the separation between the two voltage contacts. Relative changes of ρ as a function of T and H_{ext} were determined with a much higher precision, up to $\sim 0.05\%$ in some cases. The Hall constant R at high fields was measured with an absolute accuracy of several percent. Again, the precision was much higher than the accuracy. The absolute accuracy of the Hall mobility $\mu = R/\rho$ was limited by the uncertainties in ρ and R, and also by a possible nonuniformity of the carrier concentration in each sample. We estimate that the mobilities in Table I are accurate to within a factor of 2.5. All error bars in the figures of this paper represent the precision of the measurements, rather than their absolute accuracy.

Measurements of the magnetization M and the differential susceptibility dM/dH_{ext} with respect to the external (applied) magnetic field H_{ext} were made using the techniques described in Ref. 3. Temperature measurements were performed as in Ref. 3, except that a calibrated germanium resistance thermometer was used in addition to platinum and carbon resistance thermometers.

C. Magnetic fields and demagnetization corrections

All electrical transport measurements were carried out in a Bitter-type solenoid capable of generating a magnetic field of 150 kOe. For measurements at low fields, up to 3.5 kOe, a 500-A current supply replaced the 22 000-A supply of the magnet facility. Most measurements were performed with the external magnetic field $\vec{H}_{ext}$ perpendicular to the long dimension of the sample, i.e., $\vec{H}_{ext} \parallel [100]$ and $\vec{I} \parallel [010]$, where $\vec{I}$ is the electrical current in the sample. This configuration for $\vec{H}_{ext}$ and $\vec{I}$ should be assumed throughout this paper unless explicitly stated otherwise. The magnetization measurements were made either in the Bitter-type solenoid or in a superconducting magnet.

In analyzing the electrical transport data (especially the Hall data) it was sometimes necessary to know the internal magnetic field H_{int}, or the magnetic induction $B = H_{int} + 4\pi M$ inside the sample. To obtain H_{int} or B from the external field H_{ext}, we applied demagnetization corrections as discussed in Ref. 3. The values for M used in calculating these corrections were taken from magnetization data on the same sample, obtained with the same orientation of $\vec{H}_{ext}$ relative to the sample as in the electrical transport measurements.

III. MAGNETIC ORDER IN EuSe

Knowledge of the magnetic order in EuSe is important for understanding the electrical transport properties. The great complexity in the magnetic order of pure EuSe results from the comparable strengths of the ferromagnetic and antiferromagnetic interactions in this material. Further complications in the magnetic order arise in samples which contain a sufficient number of conduction or localized electrons, because these additional electrons lead to an indirect interaction between the spins of the Eu^{++} ions.[1,18] We first discuss the magnetic order in pure EuSe.

A. Magnetic phase diagram for pure EuSe

Pure stoichiometric EuSe exhibits several different magnetic phases. The magnetic phase diagram of EuSe, in the H-T plane, has been the subject of several investigations. Some of the more recent results are presented in Refs. 19–26. After summarizing these results we shall discuss some of our own data for the nonconducting sample whose magnetic behavior is assumed to approximate that of pure EuSe.

Figure 1 shows the results of Griessen et al.[19] for the magnetic phase diagram. At zero magnetic field there are three magnetic phases: (i) Between 4.6 and 2.8 K the material is antiferromagnetic (AF-I), with spins in consecutive {111} planes arranged in the sequence NNSS (i.e., ↑↑↓↓). The transition at the Néel temperature $T_N = 4.6$ K is of first order.[21] (ii) Between 2.8 and 1.8 K the material is ferrimagnetic, with an NNS(↑↑↓) sequence for the spins in consecutive {111} planes. The magnetization (in a single domain) for this phase is $\sim \frac{1}{3}$ of the saturation magnetization M_0. (iii) Below 1.8 K the order is antiferromagnetic (AF-II) and is presumed to be similar to the order in MnO and EuTe, i. e., NSNS (↑↓↑↓). If the magnetic field is increased
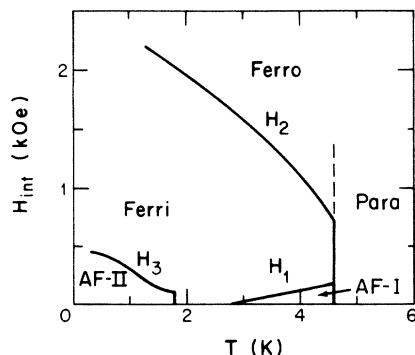
FIG. 1. Magnetic phase diagram of pure EuSe as a function of temperature T and internal magnetic field H_{int}. (After Griessen *et al.*, Ref. 19. With permission of the authors and Pergamon Press.)

from zero, the AF-I and AF-II phases transform first into the ferrimagnetic phase (at fields H_1 and H_3, respectively) and then into the ferromagnetic phase at a field H_2.

The phase diagram in Fig. 1 may be an oversimplification. Everett and Jones[23] found that below T_N the temperature variation of the anisotropy constants at $H_{int} = 4$ kOe exhibited anomalies which, in their view, were not consistent with a simple ferromagnetic phase for fields $H_{int} > H_2$. Later, Kwon and Everett[24] found that at 1.3 K the magnetization did not become saturated in internal fields as high as 19 kOe, which was regarded as additional evidence that between H_2 and 19 kOe the sample did not have a simple ferromagnetic order. The same authors also studied the effects of uniaxial stress on the magnetic order and compared their results with the theory of Janssen.[25] Komaru *et al.*[26] found that when the temperature and/or magnetic field were cycled, the magnetic phase transitions in their samples exhibited hysteresis effects. In addition, they reported the existence of an intermediate phase, in finite magnetic fields, between the "ferrimagnetic" and the "ferromagnetic" phases.

In the present work magnetization and differential susceptibility measurements were performed on the nonconducting sample which presumably approximated pure EuSe. The results were similar to those reported by earlier investigators. The zero-field differential susceptibility $\chi_0 = (dM/dH_{ext})_0$ as a function of temperature (Fig. 2) was qualitatively similar to that observed by Schwob (Ref. 20, Fig. 13) and Griessen *et al.* (Ref. 19, Fig. 4). The Néel temperature, taken from the peak in χ_0, was 4.6 ± 0.2 K. The larger peak in χ_0, near 2 K, is due to the ferrimagnetic phase (see Fig. 1). The magnetic-field dependence of the magnetization $M(H_{ext})$ showed transitions from the antiferromagnetic phases to the "ferrimagnetic" and "ferromagnetic" phases at fields comparable to those reported previously.

At 1.14 K, $M(H_{ext})$ varied by less than $\sim 0.5\%$ between 13 and 55 kOe, with a saturation value $M(55$ kOe$) = 165 \pm 3$ emu/g $= (6.82 \pm 0.12)\mu_B/Eu^{++}$ ion, compared to the theoretical saturation value $M_0 = 7\mu_B/Eu^{++}$ ion. At 4.2 K, M did not reach saturation even at 53 kOe, and $M(53$ kOe$)$ was $\sim 2\%$ below saturation.

In summary, it appears that the main features of the magnetic phase diagram of pure EuSe are given by Fig. 1, except that the phase above H_2 may not be a simple ferromagnetic phase. In addition, hysteresis effects may occur in some samples.

B. Effects of electrons on magnetic order

1. Theoretical concepts

In doped, nonstoichiometric, or defect-containing samples of the Eu chalcogenides there are additional conduction or localized electrons which are not present in pure samples. These additional electrons affect the magnetic order because the s-f coupling of the spin of an electron with different Eu^{++} ions leads to an indirect interaction between these ions. A number of possible situations, leading to different
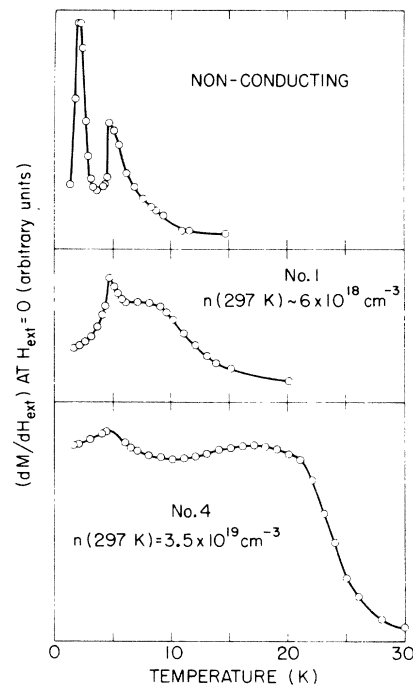

FIG. 2. Temperature variation of the zero-field differential susceptibility $\chi_0 = (dM/dH_{ext})_0$ for three EuSe samples with different carrier concentrations. The modulation field in each case was parallel to the long axis of the sample. The data were taken while the samples were cooled slowly in zero magnetic field. The results for the highest values of χ_0 (e.g., for sample 4 below ~ 20 K) were influenced by the demagnetizing field. The ordinate scales differ from sample to sample. Note that for the two conducting samples, 1 and 4, χ_0 vs T exhibits a shoulder above $T_N = 4.6$ K.

microscopic spin configurations, have been discussed
in the literature. Some of these are reviewed
briefly here, and further discussions are given in
the following sections when appropriate. It should
be noted that in the case of EuSe, for which the free-
energy differences between different types of mag-
netic order are small, the additional indirect inter-
action due to electrons may change the type of mag-
netic order. It should also be noted that it is not
always possible to conclude on the basis of magne-
tization measurements alone which of several alter-
native microscopic spin configurations is the cor-
rect one.

It is useful to distinguish between situations in
which the additional electrons are conduction elec-
trons with extended wave functions, and situations
in which the electrons are localized. This distinc-
tion is particularly important for understanding elec-
trical transport data because localized electrons are
much less effective in electrical conduction.

The two principal interactions which tend to local-
ize electrons in a magnetic semiconductor are the
Coulomb attraction to the impurities and, under
certain conditions, the s-f interaction. Three cases
may be distinguished: (a) when for a given T and
H the combined action of the Coulomb attraction
and the s-f interaction is insufficient to localize
the electron, the electron remains in the conduction
band; (b) when for a given T and H the Coulomb at-
traction by itself is insufficient to localize the elec-
tron, but the additional s-f interaction succeeds in
localizing (or trapping) the electron; (c) when the
Coulomb attraction (by itself) is strong enough to
localize the electron (i.e., the case of deep donors).
We consider cases (a) and (c) first, and then
case (b).

Conduction electrons in the paramagnetic phase
are expected to increase the susceptibility (uniformly
throughout the crystal) relative to that of the pure
crystal. The Curie-Weiss temperature Θ may then
increase. If the material is ferromagnetic, the
Curie temperature T_C may increase due to the con-
duction electrons, and the spontaneous magnetization
at $0 < T < T_C$ may be higher than in a pure material.
For an antiferromagnet below T_N, conduction elec-
trons may lead to the canting of the two sublattice
magnetizations, resulting in a spontaneous magnet-
ic moment.[27]

Consider next an electron which is bound to a deep
donor. We assume that the electron's wave function
has some overlap with the neighboring Eu^{++} ions.
In this case the s-f interaction tends to polarize the
Eu^{++} spins in the vicinity of the donor. In the pa-
ramagnetic phase this results in a cluster of ferro-
magnetically aligned Eu^{++} spins near the impuri-
ty.[12-15,28] The degree of spin alignment in the clus-
ter increases as the temperature decreases toward
the magnetic-ordering temperature. The impurity

plus spin cluster complex is called the "magnetic
impurity state" (MIS).[12-15] The existence of spin
clusters would lead to an increase in the paramag-
netic susceptibility. Similarly, in an antiferromag-
netic crystal below T_N, the presence of deep donors
may lead to the formation of ferromagnetic spin
clusters surrounded by antiferromagnetic regions.[29]

So far we discussed cases (a) and (c) involving,
respectively, conduction electrons and electrons
bound to deep donors. We now turn to case (b) in
which the donors are sufficiently shallow that they
would have been ionized in the absence of the s-f
interactions, i.e., the electrons would have been
in the conduction band were it not for the s-f inter-
action. However, the additional s-f interaction
causes the electrons to become localized. Two
situations may be distinguished: (i) when the elec-
tron becomes localized near one of the shallow do-
nors a "bound magnetic polaron" (BMP) is formed.[30,31]
(ii) When an electron becomes localized in an im-
purity-free region, a "magnetic polaron" is formed.
Magnetic polarons in the paramagnetic phase of a
ferromagnet, and in an antiferromagnet below T_N,
have been discussed in the literature.[11,15,27,29,32-34]
In a ferromagnet the conditions for the formation
of either BMP's or magnetic polarons are most
favorable near T_C. When a BMP or a magnetic
polaron is formed, the localized electron polarizes
the Eu^{++} ions in its vicinity, giving rise to a ferro-
magnetic spin cluster. These clusters enhance the
magnetic susceptibility.

Magnetic polarons and BMP's can exist only over
a limited range of temperatures and magnetic fields.
In particular, they should disappear when the Eu^{++}
spins in the entire crystal become ferromagnetically
aligned. Thus at zero magnetic field, the magnetic
polarons and BMP's cannot exist in a ferromagnet
at $T \ll T_C$, whereas in an antiferromagnet they may
persist down to $T = 0$. In general, the application
of a magnetic field, which increases the ferromag-
netic order in the entire crystal, tends to destroy
the magnetic polaron and BMP.

2. Results and discussion

Magnetization and differential susceptibility mea-
surements were performed on sample 1 which was
cut from crystal No. 1 but was not used in the elec-
trical measurements [estimated carrier concentra-
tion $n(297 \text{ K}) = 6 \times 10^{18}$ electrons/cm³ within a factor
of 2], and on sample 4 which was used in the elec-
trical measurements [$n(297 \text{ K}) = 3.5 \times 10^{19}$ electrons/
cm³]. The zero-field differential susceptibility χ_0
$= (dM/dH_{ext})_0$ vs T for sample 1 is shown in Fig. 2.
These results were obtained when the sample was
cooled in zero external magnetic field. A peak in
χ_0 was observed at $T_N = 4.6$ K, as in the nonconduct-
ing sample, indicating a transition into an antifer-

romagnetic phase. However, in contrast to the non-conducting sample, χ_0 exhibited a distinct "shoulder" near 8 K which we attribute to the presence of electrons in sample 1. In addition, the susceptibility below 3 K was qualitatively different for sample 1 than for the nonconducting sample, suggesting the absence of a ferrimagnetic phase for sample 1, i.e., the sample was antiferromagnetic between 1.5 and 4.6 K. However, because the susceptibility of sample 1 showed hysteresis when the sample was cycled in a magnetic field below 4 K, the absence of a ferrimagnetic phase is not certain.

The magnetization vs H_{ext} for sample 1 at 4.2 K was qualitatively similar to that of the nonconducting sample, and showed the low-field transitions to the "ferrimagnetic" and "ferromagnetic" phases. At 4.2 K, $M(H_{ext})$ became saturated only in fields above ~ 80 kOe, and the saturation moment was

$$M_0 = 167 \pm 3 \text{ emu/g} = (6.9 \pm 0.1)\mu_B/\text{Eu}^{++} \text{ ion}$$

(see Fig. 3). Magnetization measurements at temperatures up to 250 K gave a paramagnetic Curie-Weiss temperature $\Theta \cong 11$ K for this sample.

For sample 1, the shoulder which χ_0 exhibits near 8 K may be due to ferromagnetic spin clusters which are formed when the electrons become localized. Near 4.6 K those regions of the sample which are not near the localized electrons are magnetically similar to pure EuSe, as indicated by the antiferromagnetic transition at this temperature.

For sample 4, χ_0 vs T (Fig. 2) showed a shoulder near 20 K. This shoulder was much more pronounced than for sample 1 with the lower carrier concentration. A small peak in χ_0 was observed also in sample 4 near 4.6 K. The low-field magnetization at liquid-helium temperatures (Fig. 4) was similar to that of a ferromagnet with a spontaneous
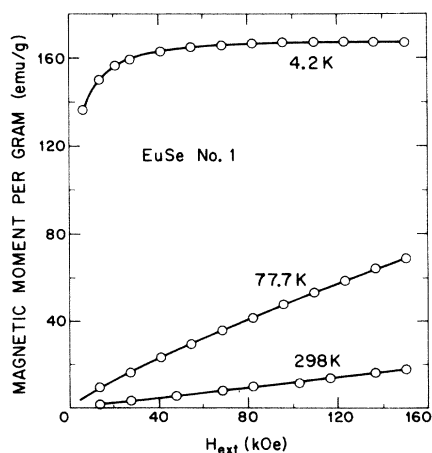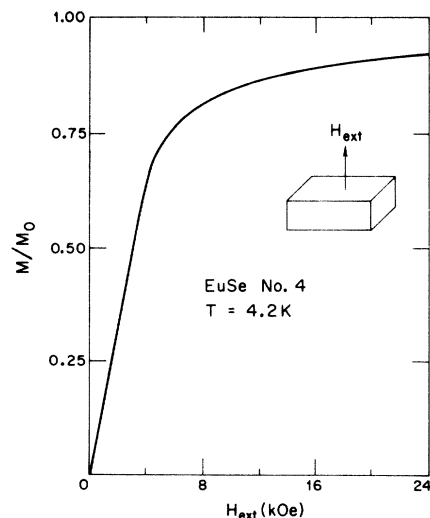

FIG. 4. The reduced magnetization M/M_0 of sample 4 as a function of H_{ext} at 4.2 K. The data were taken with $\vec{H}_{ext}$ perpendicular to the long axis of the sample (demagnetizing factor $N \cong 6$).

magnetic moment at zero field, and the data did not show the field-induced transitions observed in pure EuSe. (The data in Fig. 4 were taken with the long axis of the sample perpendicular to $\vec{H}_{ext}$, and are displayed for a later comparison with resistivity data. Magnetization data taken with $\vec{H}_{ext}$ parallel to the long axis of the sample were qualitatively similar except that $\chi_0 = (dM/dH_{ext})_0$ was higher, as expected for a lower demagnetizing factor.)

The spontaneous magnetization M_s in a single domain of a low-anisotropy ferromagnet is very roughly given by the value of $M(H_{ext})$ at the beginning of the "knee" in the M-vs-H_{ext} curve. On this basis, Fig. 4 gives $M_s \cong 0.6M_0$ for sample 4 at 4.2 K. Other data for sample 4 showed that a spontaneous magnetic moment first appeared near 21 K and increased monotonically with decreasing T down to 1.5 K. At 4.2 K the magnetization became saturated or very nearly saturated at ~ 90 kOe, with a saturation magnetic moment $M_0 = 167 \pm 3$ emu/g. At 1.65 K the magnetization was saturated, or very nearly saturated, above ~ 60 kOe. The paramagnetic Curie-Weiss temperature was $\Theta \cong 26$ K.

The above data for sample 4 suggest that ferromagnetic spin clusters are already formed at 21 K, and that the number of such clusters and/or their size increases at T decreases. Below 4.2 K these ferromagnetic clusters fill most of the volume of the sample and the magnetic behavior is dominated by them. However, near 4.6 K some parts of the sample undergo an antiferromagnetic transition, characteristic of pure EuSe. If one assumes that the number of clusters is roughly equal to $n(0, 297$ K$) \cong n(100$ kOe, 4.2 K$)$, the spontaneous magnetic

FIG. 3. Magnetization of sample 1 vs external (applied) magnetic field H_{ext} at three temperatures. The average demagnetizing factor is approximately equal to 6.

moment at 4.2 K corresponds to several hundred Eu^{++} ions per cluster. A similar value for the magnetic moment per electron was obtained for the spin clusters in antiferromagnetic EuTe.[35]

In summary, the low-temperature magnetic properties of samples 1 and 4 are interpreted in terms of ferromagnetic spin clusters surrounded by regions which become antiferromagnetic at the Néel temperature of pure EuSe. In sample 1 the volume of the regions outside the clusters is larger than the total volume of the clusters, whereas the opposite is true for sample 4 at the lowest temperatures. Although this picture for the microscopic magnetic order is based on limited macroscopic data, it accounts for many of the electrical transport properties in addition to the results for M and χ_0.

IV. GENERAL FEATURES OF RESISTIVITY DATA

To set the stage for a detailed discussion of the resistivity and Hall data, we first briefly describe their main features. Each of these features will then be examined in detail in a separate section.

Carried concentration and mobility. Table I show that at room temperature the electron concentration $n(297\ \text{K})$ varies from 4.2×10^{18} to 3.5×10^{19} cm^{-3}, and the Hall mobility $\mu(297\ \text{K})$ ranges from 20 to 51 cm^2/V sec. As noted earlier these values of μ are accurate within a factor of about 2.5 so that the differences in the quoted mobilities for different samples are not necessarily significant.

Resistivity peak. The T dependence of $\rho(H_{\text{ext}}, T)$ at several fixed values of H_{ext} is shown for three samples in Figs. 5–7. These three figures are for successively lower carrier concentrations. The
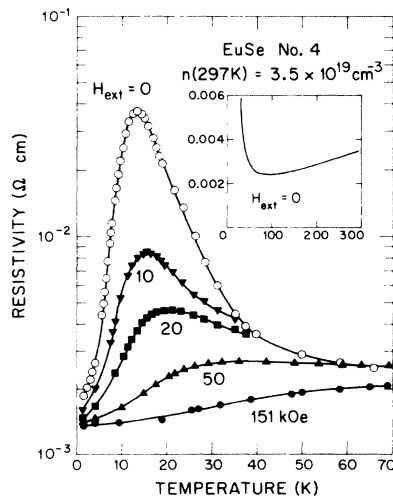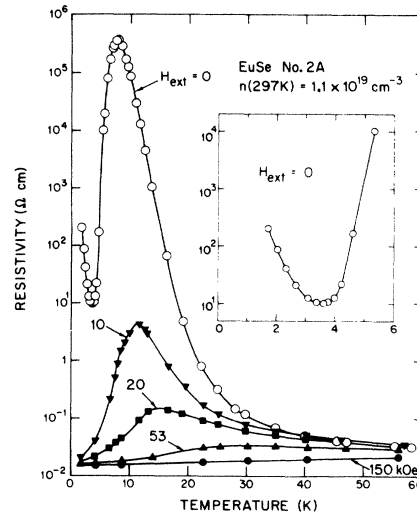

FIG. 6. Resistivity of sample 2A vs T for several fixed values of H_{ext}. The insert shows the zero-field resistivity vs T at *low* temperatures.

most prominent feature in each case is the large peak in the zero-field resistivity $\rho(0, T)$. This peak was observed earlier by von Molnar and Methfessel[9] in Gd-doped EuSe. A similar peak was also ob-
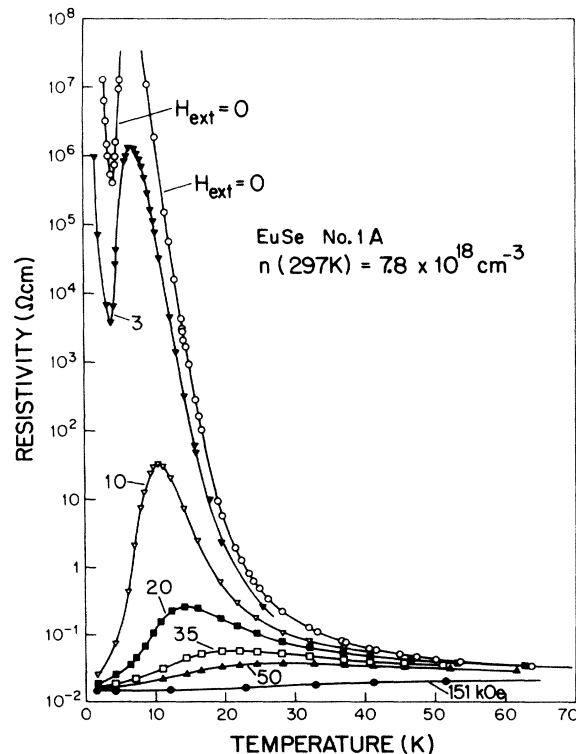

FIG. 5. Resistivity of sample 4 vs temperature T for several fixed values of H_{ext}. The insert shows the zero-field resistivity vs T at *high* temperatures.

FIG. 7. Temperature variation of the resistivity of sample 1A for several fixed values of H_{ext}.

served in EuO and EuS near the Curie temperature
(see Refs. 3–5 and literature cited there), but not
in antiferromagnetic EuTe.[6] The temperature
where $\rho(0, T)$ is maximum will be called T_{max}.

Negative magnetoresistance. Figures 5–7 also
show the existence of an extremely large negative
magnetoresistance. A magnetic field tends to sup-
press the resistivity peak. In addition, as H_{ext} in-
creases, the resistivity peak shifts to a higher tem-
perature and becomes broader.

Low-temperature behavior. In samples 1A and
2A, as T decreased from T_{max} to 1.6 K, $\rho(0, T)$
first decreased rapidly, then went through a mini-
mum, and finally increased (Figs. 6 and 7). A sim-
ilar behavior was also observed in all other samples
which were studied in this temperature range, except
for sample 4 which had the highest carrier concen-
tration. In sample 4, $\rho(0, T)$ decreased monotonically
with decreasing T between T_{max} and 1.6 K (Fig. 5).

Positive magnetoresistance. A close examination
of Fig. 6 reveals another phenomenon. Above 40 K
the resistivity for $H_{ext} = 10$ kOe is higher than the
zero-field resistivity, indicating the existence of a
positive magnetoresistance at low fields in a lim-
ited temperature range.

V. METHOD OF ANALYZING HALL DATA

The purpose of the Hall measurements was to
determine the carrier concentration n as a function
of T and H_{ext}. In magnetic materials the main
complication in determining n from the measured
Hall voltage V_H is the possibility of the existence
of an "anomalous" Hall voltage in addition to the
"ordinary" (or "normal") Hall voltage. In general,
the Hall voltage in a magnetic material is given by
the relation

$$V_H = (R_0 B + R_1 M)(I/t), \qquad (1)$$

where R_0 is the ordinary Hall coefficient which is
related to n in the standard way, $B = H_{int} + 4\pi M$ is
the magnetic induction inside the sample, R_1 is the
anomalous Hall coefficient, I is the electrical cur-
rent, and t is the thickness of the sample along $\vec{H}_{ext}$.
To determine R_0 from V_H one must separate the
contributions of the ordinary and anomalous Hall
terms. In many magnetic materials the anomalous
term cannot be neglected.

The procedure used to obtain R_0 from V_H was
discussed in detail in the work on EuO.[3] This pro-
cedure is based on results of Hall measurements
for cases where R_0 and R_1 are expected to be mag-
netic-field independent. In these cases the ordinary
term $R_0 B$ can be separated from the anomalous term
$R_1 M$. For EuO it was found that $R_1 M \ll R_0 B$, i.e.,
V_H was given by the expression

$$V_H = R_0 B I/t. \qquad (2)$$
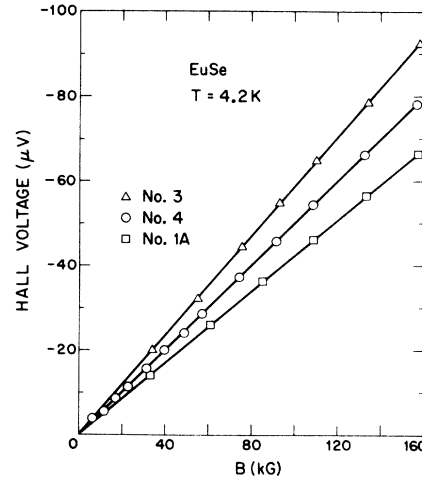
On this basis it was assumed in Ref. 3 that the anom-

FIG. 8. Hall voltage vs magnetic induction $B = H_{int}$
$+ 4\pi M$, at 4.2 K. The measuring current and sample
thickness are different for each of the three samples.

alous Hall term in EuO was negligible in all cases,
including those where R_0 was magnetic-field depen-
dent.

The dependence of V_H on B for three EuSe samples
at 4.2 K is shown in Fig. 8. Similar data were ob-
tained for other samples at 4.2 K, and also at 1.6 K.
The data show that at fields above several kG, V_H
is proportional to B. Of particular importance is
the fact that the data for V_H vs B in fields above
~ 85 kG lie on a straight line whose extrapolated
intercept with the V_H axis is very near the origin.
At these high fields the magnetization M is practically
saturated (see Fig. 3), and therefore R_0, R_1, and
$R_1 M$ are all expected to be constant. Hence, the
high-field data show that $R_1 M \ll R_0 B$, because other-
wise the straight line for V_H vs B would not pass
through the origin [see Eq. (1)]. On this basis *we
shall assume throughout this work that in all cases
the anomalous Hall term $R_1 M$ is negligible com-
pared to the ordinary term $R_0 B$.* The coefficient
$R_0(H_{ext}, T)$ will be calculated from V_H using Eq. (2).

Figure 3 shows that at room temperature the
magnetization in EuSe was linear with H_{ext}, with
$M/H_{ext} \cong 8 \times 10^{-4}$. It follows that in this case B
$= a H_{ext}$, where a is a constant which differs from
unity by less than 1%. In these circumstances the
ordinary Hall coefficient R_0 calculated from Eq. (2)
is practically equal to the Hall coefficient R calcu-
lated from the standard formula for nonmagnetic
semiconductors, viz.,

$$V_H = R H_{ext} I/t. \qquad (3)$$

At low temperatures, however, R_0 can differ appre-
ciably from R because $4\pi M$ is often not negligible
compared to H_{ext}.

Unless otherwise specified the carrier concentra-
tion n will be calculated from R_0 using the relation

$n = 1/R_0 e$. This relation is valid for a single conduction band under the assumption that the Hall factor r (defined by the exact expression $n = r/R_0 e$) is equal to unity. As in the case of EuO,[3] whenever M is nonzero the conduction band of EuSe is split into two subbands, for spin up and spin down, and this splitting can lead to two-band conduction (another such situation is discussed in Sec. VI). However, even in the case of two-band conduction the value of n calculated on the assumption of a single band is not seriously in error unless the mobilities in the two bands differ appreciably. The exceptional situations where the relation $n = 1/R_0 e$ may be seriously in error will be pointed out explicitly. The effects of spin splitting of the conducting band on R_0, as well as other H-induced changes of R_0, are discussed in the following paper.[16]

The only mobility determined in the present work is the Hall mobility μ defined as $\mu = R_0/\rho$.

VI. CONDUCTIVITY NEAR ROOM TEMPERATURE

The most extensive theoretical interpretation of the early electrical transport data in EuSe[7-9] and EuS[36] is the one advanced by Kasuya, von Molnar, and co-workers.[10-15] Fundamental to this interpretation is the distinction between heavily doped samples in which electrical conduction takes place in a band, and samples with low concentration of impurities in which conduction takes place by a hopping process between localized impurities. von Molnar estimated theoretically that the transition from hopping conduction to band conduction takes place at an impurity concentration of about $5 \times 10^{20}/\mathrm{cm}^3$, but found experimentally that this estimate was too high.[10] Kasuya and Yanase[12-15] considered the case of hopping conduction in detail. According to their theory an electron localized near a deep donor aligns the spins of the Eu^{++} ions in its neighborhood, leading to the formation of the MIS. Conductivity in this case is governed by an activation energy for hopping which depends on the magnetic order in the sample.

To interpret our data it is important to decide first whether conduction near room temperature is band conduction or thermally-activated hopping conduction. The results in Table I show that the room-temperature Hall mobilities are equal to 30 cm^2/V sec, within a factor of 2. These mobilities are close to those in the conduction band of Eu-rich EuS single crystals with comparable carrier concentrations.[37] In addition, the data in the insert of Fig. 5 show that near room temperature the zero-field resistivity of sample 4 increases with increasing T. This is expected for band conduction for which the high-temperature mobility is reduced by phonon scattering, but is inconsistent with a thermally activated hopping conduction. Similar data

to those in the insert of Fig. 5 were also obtained for samples 3 and 1B which had lower carrier concentrations. [However, the temperature where $\rho(0, T)$ was minimum increased with decreasing n.] We interpret these results to mean that *near room temperature* electrical conduction in all of our samples took place in the conduction band. It is possible that this conduction band had a "tail" similar to the one for EuS discussed by Thompson *et al.*[37]

In interpreting the transport properties of Gd-doped EuSe, Yanase and Kasuya paid considerable attention to the results for a single-crystal of $\mathrm{Eu}_{0.99}\mathrm{Gd}_{0.01}\mathrm{Se}$ which was studied by von Molnar and Methfessel.[9] Room-temperature Hall measurements on this sample gave $n = 1/Re = 3.1 \times 10^{18}$ electrons/cm^3, and a Hall mobility $\mu = 15$ cm^2/V sec. According to Yanase and Kasuya[12] the room-temperature conductivity in this sample was due mainly to hopping between localized states, with a much smaller contribution from band conduction. Their model involved conduction in two bands: n_1 carriers in the conduction band with mobility μ_1, and n_2 hopping electrons with mobility μ_2. The resistivity and Hall coefficient in this case are given by

$$\rho^{-1} = n_1 e \mu_1 + n_2 e \mu_2 \quad , \tag{4}$$

and

$$R = (n_1 \mu_1^2 + n_2 \mu_2^2)/e(n_1 \mu_1 + n_2 \mu_2)^2. \tag{5}$$

It was assumed that in Eq. (4), $n_2 \mu_2$ was much larger than $n_1 \mu_1$ because $n_2 \gg n_1$. However, the Hall voltage was assumed to be due mainly to band electrons, i.e., $n_1 \mu_1^2 \gg n_2 \mu_2^2$ because $\mu_1 \gg \mu_2$. In this case

$$R = n_1 \mu_1^2/e(n_1 \mu_1 + n_2 \mu_2)^2. \tag{6}$$

Using Eq. (6) the binding energy of the impurity level was calculated assuming: (a) that the number of impurities in the sample was given by the nominal value for the Gd concentration, and (b) that the product $n_1 \mu_1$ could be taken from the conductivity of another sample which was polycrystalline, but with the same nominal Gd concentration. Both of these assumptions are questionable. Generally, the concentration of impurities incorporated in a sample can be quite different from the nominal doping level, and differences between two samples with the same nominal impurity concentration can arise for reasons other than difference in the degree of compensation, as assumed by Yanase and Kasuya.

Setting aside the question of whether the binding energy of the impurity was correctly obtained in Ref. 12, we examine the possibility that the two-band model with $n_2 \mu_2 \gg n_1 \mu_1$ and $n_1 \mu_1^2 \gg n_2 \mu_2^2$ applies to *our* samples at room temperature. We note that n_1 varies exponentially with the binding energy of the impurity divided by kT, and that μ_2 is governed by the activation energy for hopping conduction.
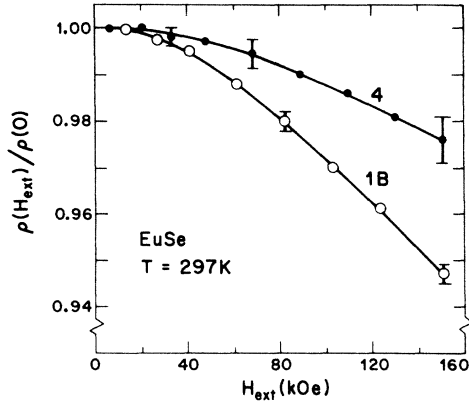
FIG. 9. Dependence of the normalized resistivity $\rho(H_{ext})/\rho(0)$ on H_{ext} at 297 K for samples $1B$ and 4. Some typical experimental uncertainties are shown.

From Eqs. (5) or (6) we therefore expect that if the above two-band model were applicable then R would be strongly dependent on T and/or H_{ext}. However, the results in Table I and those in the following sections indicate that R was not strongly dependent on T or H_{ext} [except, possibly, when both $T \lesssim 3T_{max}$ and $H_{ext} \lesssim 10$ kOe, i.e., near the resistivity peak and at low fields]. Moreover, as already noted, the resistivity near room temperature increased with increasing T, whereas the opposite is expected for hopping conduction. We conclude that near room temperature both the conductivity and Hall effect in our samples were due to band electrons.

VII. NEGATIVE MAGNETORESISTANCE AT $T \gg T_{max}$

A. Experimental results

The room-temperature magnetoresistance in fields up to 150 kOe was measured for seven of the ten samples. The results for all samples, except sample 4, were quantitatively similar to those for sample $1B$ in Fig. 9. The magnetoresistance was negative, and was equal to -5% at 150 kOe. In sample 4, which had the highest carrier concentration, the negative magnetoresistance was significantly smaller (see Fig. 9).

At room temperature the Hall coefficient $R(H_{ext})$ did not vary by more than a few percent between ~ 30 and 150 kOe. However, with most samples the precision was insufficient to determine the relative contributions of n and μ to the change in the resistivity ρ. The clearest case was that of sample $1B$ for which $R(H_{ext})$ did not show any systematic change greater than $\sim 2\%$ between 25 and 150 kOe (see Fig. 10). Over the same field range ρ changed by 5%, suggesting that at least a large part of the negative magnetoresistance was due to an increase in μ. We note that for EuO samples with comparable carrier
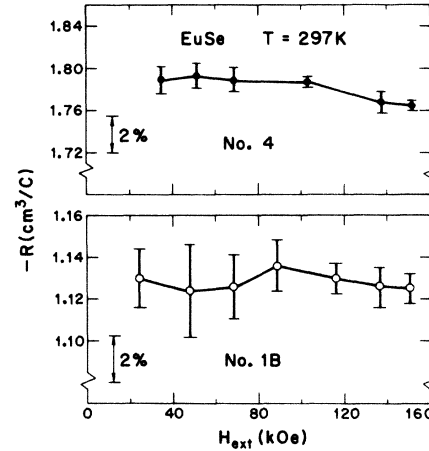

FIG. 10. Hall coefficient R at 297 K vs H_{ext} for samples $1B$ and 4. Note the breaks in the ordinate scales. The magnitude of a 2% change in R is indicated for each case.

concentrations μ increases by $\sim 25\%$ when a magnetic field of 140 kOe is applied at room temperature.[3]

The negative magnetoresistance at high fields increased in magnitude as T decreased. This is illustrated by the results for sample 4 in Fig. 11 (the positive magnetoresistance at low fields observed in this figure will be discussed separately in Sec. VIII). Results for $\rho(H_{ext})$ and for the ordinary Hall coefficient $R_0(H_{ext})$ for samples $1A$, 3 and 4 at 77.7 K are shown in Figs. 12 and 13, respectively. For all three samples $R_0(H_{ext})$ decreased slowly with increasing H_{ext} above ~ 30 kOe. However, this decrease in R_0 was small compared to the decrease in ρ. For example, in sample $1A$, R_0 decreased by $(5.1 \pm 2.6)\%$ between 35 and 150 kOe,
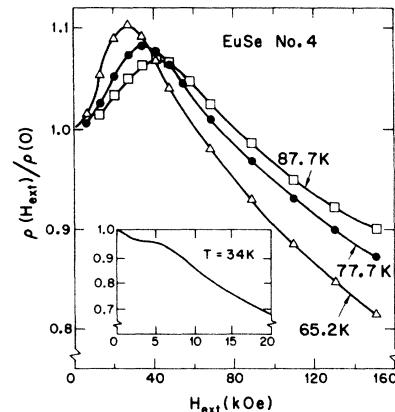

FIG. 11. Variation of $\rho(H_{ext})/\rho(0)$ with H_{ext} for sample 4 at 65.2, 77.7, and 87.7 K. The insert shows $\rho(H_{ext})/\rho(0)$ vs H_{ext} at 34 K.
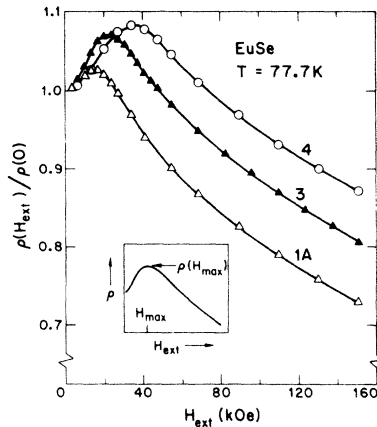
FIG. 12. $\rho(H_{ext})/\rho(0)$ vs H_{ext} for samples 1A, 3, and 4 at 77.7 K. The sketch in the insert defines H_{max} and $\rho(H_{max})$.

whereas ρ decreased by 25%. This indicates that at 77.7 K the negative magnetoresistance at high fields is primarily due to an increase in the mobility. Similar results were obtained for EuS at 77.7 K.[5]

B. Discussion

The assumption $R_0 = \text{const } n^{-1}$, where n is the total number of carriers is valid only for a single band when the Hall factor r is a constant. This assumption is not strictly valid for a changing magnetic field. The H-dependence of r is examined in Sec. III F of the following paper.[16] The calculations suggest that the change in r is not appreciable. Hence, the conclusion that the negative magnetoresistance at high fields is primarily due to a change in μ remains valid.

In Sec. VI we interpreted electrical conduction at $T \gg T_{max}$ as band conduction. In this case the s-f (or d-f) interaction between the spins of the conduction electrons and those of the Eu^{++} ions leads to "spin-disorder scattering." This scattering was considered by Kasuya,[38] and later by others (see Sec. IV of Ref. 2, and literature cited there). It is important to note that spin-disorder scattering persists well above the magnetic ordering temperature, and that it disappears only when all the Eu^{++} spins are completely aligned, i.e., at low temperatures and/or high magnetic fields.

The effect of a magnetic field on spin-disorder scattering was calculated by Haas,[2] who showed that the resulting magnetoresistance is negative. Physically, a magnetic field increases the alignment of the Eu^{++} spins, thus decreasing spin disorder. In addition, a magnetic field splits the conduction band into spin-up and spin-down subbands. Due to this splitting, scattering events in which the

electron spin reverses its direction (spin-flip scattering) are less frequent at high fields. Since spin-disorder scattering involves both spin-flip and non-spin-flip scattering events, the reduction in the number of the former also leads to a negative magnetoresistance. For a more detailed discussion see Ref. 16.

We attribute the negative magnetoresistance at $T \gg T_{max}$ to an H-induced decrease of spin-disorder scattering. At lower temperatures, comparable to or lower than T_{max}, other mechanisms may also lead to a negative magnetoresistance (see Sec. IX).

VIII. POSITIVE MAGNETORESISTANCE AT $T \gg T_{max}$

As shown in Fig. 12, at 77.7 K the magnetoresistance is positive at low fields, reaches a maximum at $H_{ext} = H_{max}$, and is negative at higher fields. A similar positive magnetoresistance was observed earlier in EuTe (Ref. 6, Fig. 4), and in some EuS samples (Ref. 5, Fig. 2), but was not studied systematically. In the present work the temperature variation of H_{max} and of $(\Delta\rho/\rho)_{max} \equiv [\rho(H_{max}) - \rho(0)]/\rho(0)$ was determined for several samples with different carrier concentrations. The results for samples 1B and 4, with carrier concentrations differing by a factor of ~6, are shown in Fig. 14. For each sample, as T decreased, H_{max} decreased. Also, as T decreased, $(\Delta\rho/\rho)_{max}$ first increased, then reached a maximum, and finally decreased rapidly towards zero. For sample 4 the positive magnetoresistance disappeared below 35 K. In the same sample the extrapolation of the H_{max}-vs-T curve to $H_{max} = 0$ gave $T \cong 29$ K. The situation be-
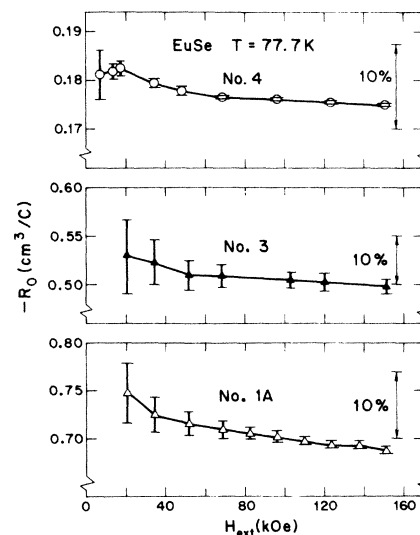

FIG. 13. Ordinary (normal) Hall coefficient R_0 vs H_{ext} for samples 1A, 3, and 4 at 77.7 K. The magnitude of a 10% change in R_0 is indicated for each sample.
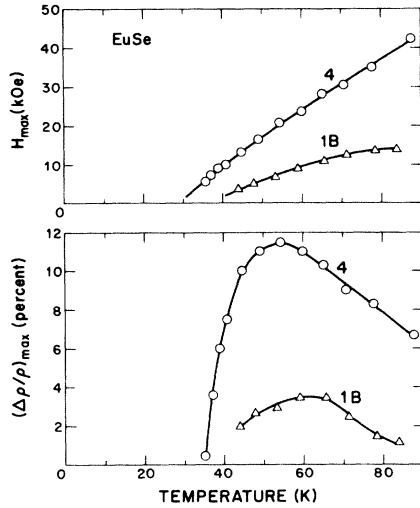
FIG. 14. Temperature variation of H_{max} and $(\Delta\rho/\rho)_{max}$ $= [\rho(H_{max}) - \rho(0)]/\rho(0)$ for samples $1B$ and 4.

tween 35 and 29 K is illustrated by the results in the insert of Fig. 11 which show a "hump" super-imposed on a negative magnetoresistance. The "hump" at this temperature occurs at a finite mag-netic field, but ρ is lower than $\rho(0)$ so that $\Delta\rho/\rho$ is negative. The results in Sec. VII show that the positive magnetoresistance did not persist up to room temperature.

Comparison of the results for several samples showed that for a fixed T, H_{max} increased with in-creasing carrier concentration. The results for $(\Delta\rho/\rho)_{max}$ were less clearcut, but samples with higher carrier concentrations usually had higher values for $(\Delta\rho/\rho)_{max}$ at a given T.

Hall measurements were carried out in an effort to determine whether the positive magnetoresistance was due to a change in the carrier concentration or to a change in the mobility. The results in most samples were inconclusive because below H_{max} the precision in determining R_0 was comparable to the percentage changes in ρ. The most precise results are those for sample 4 in Fig. 13. These Hall data suggest that the main cause for the positive mag-netoresistance in Fig. 12 was a decrease in mobil-ity. For example, between 7 and 35 kOe, the resis-tivity of sample 4 changed by $+7.5\%$ whereas R_0 changed by $(-1 \pm 3)\%$. This implies a decrease of $(8.5 \pm 3)\%$ in the Hall mobility.

Usually the magnetoresistance observed in the Eu chalcogenides is negative. Therefore, the exis-tence of a positive magnetoresistance, even in a limited temperature and magnetic-field range, is surprising.' This positive magnetoresistance is too large to be explained in terms of the classical posi-tive magnetoresistance observed in many semicon-ductors.[39] The classical magnetoresistance $(\Delta\rho/ \rho)_{class}$ is of the order $(\mu H_{ext})^2$, which for $\mu < 100$ cm^2/

V sec and $H_{ext} < 40$ kOe gives $(\Delta\rho/\rho)_{class} \lesssim 10^{-3}$, where-as some of the results in Figs. 11 and 12 show $(\Delta\rho/\rho)_{max} \sim 10^{-1}$.

A model for the positive magnetoresistance is presented in the following paper.[16] The model focuses on effects resulting from spin splitting of the conduction band.

IX. RESISTIVITY PEAK AT T_{max}

A. Experimental results

The large peak in the zero-field resistivity $\rho(0, T)$ vs T is shown in Figs. 5–7. The data in Table I suggest that the temperature T_{max} [where $\rho(0, T)$ is maximum] increases with increasing carrier con-centration n. Furthermore, the magnitude of the resistivity peak seems to decrease rapidly with increasing n. A peak in $\rho(H_{ext}, T)$ vs T is also ob-served for a finite fixed H_{ext}, but as H_{ext} increases the peak becomes smaller and shifts to higher tem-peratures.

Hall measurements from 4.2 K to temperatures well above T_{max} were made on samples $1A$ and 4. For experimental reasons these measurements were confined to $H_{ext} \geq 20$ kOe for sample $1A$, and $H_{ext} \geq 10$ kOe for sample 4. The results for sample 4 indicated that R_0 was nearly independent of T and H_{ext} (see Fig. 15). Thus for this sample the resis-tivity peak and negative magnetoresistance at $H_{ext} \geq 10$ kOe were due to a change in μ and not to a change in n. Similar results were also obtained for sample $1A$ above 20 kOe. The less extensive Hall data of von Molnar and Methfessel[9] are con-sistent with ours.

B. Discussion

In the range of temperatures and magnetic fields where Hall measurements were performed, the
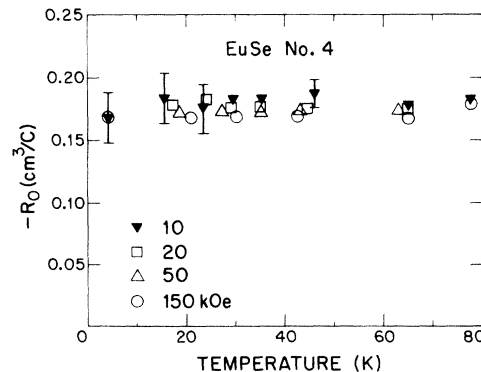

FIG. 15. R_0 vs temperature for sample 4 at several values of H_{ext}. Some of the experimental uncertainties at the lowest field are indicated. The uncertainties tend to decrease with increasing H_{ext}. For corresponding re-sistivity data see Fig. 5.

Hall mobility was higher than 3 cm^2/V sec for sample 1A, and 20 cm^2/V sec for sample 4. In this range, electrical conduction is interpreted as band conduction with a constant number of carriers, but with a mobility which is lowered by spin-disorder scattering. However, this interpretation is probably *not* valid at zero and low magnetic fields when T is near T_{max}, especially for samples with $\rho(0, T_{max})$ many orders of magnitude higher than $\rho(0, 297$ K$)$. For example, if one assumes a constant n then the zero-field mobility of sample 1A at T_{max} is lower than 10^{-7} $cm^2/$ V sec. Such a low mobility seems unreasonable for ordinary band conduction, as pointed out earlier.[9] Therefore, it appears that the very high values of $\rho(0, T)$ near T_{max} are caused by some form of electron localization. Evidence for the formation of ferromagnetic spin clusters near T_{max}, due to electron localization, was presented in Sec. III. Low-field Hall data near T_{max}, which could be used to check this interpretation directly, were not obtained for experimental reasons.

The localization of electrons may lead to the formation of either bound magnetic polarons or magnetic polarons. In the former case the electrical conductivity is expected to be due to a hopping process, and the mobility should be very low. In the case of magnetic polarons, the electron motion is expected to be diffusive, with a low mobility which Kasuya *et al.*[15] estimated to be of order 10^{-2} $cm^2/$ V sec. If one accepts this estimate then the data on samples 1A and 2A cannot be interpreted solely in terms of magnetic polarons. This would suggest that the preferred interpretation of the large resistivity peak involves bound magnetic polarons. Recently, Torrance and Holtzberg[40] have attributed the resistivity peak near the Curie temperature of EuS to the formation of bound magnetic polarons.[41]

Grigin and Nagaev[42] considered the situation when a sample contains both localized and band electrons. The ferromagnetic spin clusters associated with the localized electrons will then increase the scattering of the band electrons. Therefore, the mobility of the band electrons will be lower. This calculation may be relevant to some of our data, taken at temperatures and fields where only some of the electrons were localized.

In summary, we propose the following tentative interpretation for the resistivity peak. At $T \gg T_{max}$ electrical conduction is due to electrons in the conduction band. As T decreases toward T_{max}, $\rho(0, T)$ increases because of the increase in spin-disorder scattering. This description holds as long as the effect of the s-f (or d-f) interaction on the conduction electrons is relatively small, i.e., for mobilities which are not much smaller than 1 cm^2/V sec. At temperatures close to T_{max}, where the effects of the s-f interaction on the electrons are large, the electrons be-

come localized and form bound magnetic polarons (or, possibly, magnetic polarons). The localization of the electrons leads to a large increase in ρ. At temperatures for which the electrons are localized at zero magnetic field, the application of a magnetic field tends to delocalize them. In that case band conduction occurs only above several kOe. Thus, near T_{max} the negative magnetoresistance at low fields reflects the delocalization process, whereas the negative magnetoresistance above several kOe is due to a decrease in spin-disorder scattering of band electrons. As discussed later, the resistivity of sample 4 (with the highest carrier concentration) was least affected by electron-localization.

X. RESISTIVITY AT $T < T_{max}$

A. Zero-field resistivity

The temperature variation of $\rho(0, T)$ at $T < T_{max}$ was measured for six of the ten samples. With the exception of sample 4, as T decreased, $\rho(0, T)$ decreased rapidly below T_{max}, went through a minimum, and then increased rapidly. This behavior is illustrated by the results in Figs 6 and 7. The temperature where $\rho(0, T)$ was minimum varied from 3.4 to 4.3 K, depending on the sample. In sample 4, $\rho(0, T)$ decreased monotonically with decreasing T, from T_{max} (13.4 K) to 1.6 K (see Fig. 5).

At any fixed T near and below ~ 10 K, the value of $\rho(0, T)$ in all samples seemed to depend strongly on the high-temperature carrier concentration $n(T \gg T_{max})$. As $n(T \gg T_{max})$ increased, $\rho(0, T)$ decreased. For example, at 4.2 K the zero field resistivity of sample 4 [$n(297$ K$) = 3.5 \times 10^{19} cm^{-3}$] was ten orders of magnitude smaller than that of sample 1C [$n(297$ K$) = 4.2 \times 10^{18} cm^{-3}$] (see Table I).

For a ferromagnet one expects that below T_C bound magnetic polarons and magnetic polarons will become less stable with decreasing T. This should result in a decrease in $\rho(0, T)$. However, in an antiferromagnet, magnetically trapped (localized) electrons may still exist well below the Néel temperature.[33,34] In EuSe the magnetic order is more complicated than that of a simple ferromagnet or a simple antiferromagnet. Due to this complexity and the lack of a quantitative theory, the discussion of electron-trapping effects in EuSe is, by necessity, incomplete.

We first discuss the behavior of EuSe samples other than sample 4. Just below T_{max} the decrease of $\rho(0, T)$ with decreasing T suggests that the magnetically trapped electrons become somewhat less localized. This behavior near T_{max} is similar to that expected for a ferromagnet near T_C. For a ferromagnet, electron trapping should disappear well below T_C. However, in EuSe, $\rho(0, T)$ remains

very high at $T \ll T_{max}$, indicating that electron trap-
ping persists well below T_{max}. There are some sim-
ilarities between the behavior of $\rho(0, T)$ at $T \ll T_{max}$
and the behavior of $\rho(0, T)$ in antiferromagnetic
EuTe below T_N.[6] In both cases $\rho(0, T)$ increases
rapidly with decreasing T, suggesting a thermally-
activated hopping conduction associated with mag-
netically trapped electrons.

In sample 4, the high-temperature carrier con-
centration was significantly higher than in the other
samples. The magnetization and susceptibility
data in Sec. III showed that a spontaneous magnetic
moment appeared at ~ 21 K and was quite large at
$T \leq 4.2$ K. The spontaneous moment M_s was attrib-
uted to ferromagnetic spin clusters which, at least
below 4.2 K, filled most of the volume of the sam-
ple. This suggests that many of the spin clusters
overlapped, which enabled an electron to move from
one cluster to another. In the other samples, with
lower carrier concentrations, the concentrations of
spin clusters was lower and, therefore, the over-
lap between clusters was smaller, which resulted
in a more effective electron trapping. This accounts
for the qualitatively different behavior of $\rho(0, T)$ be-
tween sample 4 and the other samples. The data in
Sec. III show that in sample 4, M_s increased with
decreasing T, which is consistent with an increasing
overlap of the ferromagnetic spin clusters. The
increasing overlap should result in lower ρ, as ob-
served.

B. Low-field magnetoresistance

The low-field magnetoresistance for sample 4 at
4.2 K is shown in the upper part of Fig. 16. The
two sets of data are for $\vec{H}_{ext}$ perpendicular to the
long axis of the sample (demagnetizing factor
$N_\perp \cong 6$) and parallel to this axis ($N_\parallel \cong 1$). Note that
for $N_\perp$ the resistivity is independent of H_{ext} for
$H_{ext} \leq 4.5$ kOe, whereas for $N_\parallel$ the resistivity be-
gins to decrease at $H_{ext} < 1$ kOe.

For a sample with a spontaneous magnetic moment
M_s, and a small anisotropy, the internal magnetic
field H_{int} is nearly equal to zero for external fields
$H_{ext} \leq NM_s$. At 4.2 K, $M_s \cong 0.6M_0$ for sample 4, so
that $N_\perp M_s \cong 4$ kOe (see Fig. 4 and Sec. III B2). The
results in Fig. 16 for sample 4 with $N = N_\perp$ indicate
therefore that the magnetoresistance is zero as long
as $H_{int} = 0$. Since $N_\perp \gg N_\parallel$, $N_\perp M_s \gg N_\parallel M_s$ and the re-
sistivity for the configuration $N = N_\parallel$ starts to de-
crease at a much lower value of H_{ext} than for $N = N_\perp$.
The absence of a magenetoresistance for $H_{ext} < NM_s$
was observed earlier in EuO and was used to deter-
mine the Curie temperature (Ref. 3, Sec. IV C3).

In contrast to sample 4, which had an appreciable
M_s at 4.2 K, sample 1A had a small or zero M_s at
the same temperature (see Sec. III). Thus $N_\perp M_s$
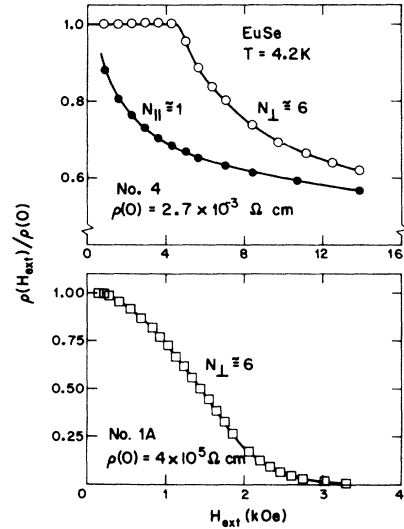was much smaller for sample 1A than for sample 4.

FIG. 16. $\rho(H_{ext})/\rho(0)$ vs H_{ext} at 4.2 K. The top figure
is for sample 4 with $\vec{H}_{ext}$ either perpendicular to the long
axis of the sample (demagnetizing factor $N_\perp \cong 6$), or paral-
el to the long axis (demagnetizing factor $N_\parallel \cong 1$). The
bottom figure is for sample 1A with $N_\perp \cong 6$. Note the dif-
ferent abscissa scales for the top and bottom figures.

This explains why in Fig. 16 the resistivity of sam-
ple 1A begins to decrease at a much lower value of
H_{ext}.

At $T \lesssim T_{max}$, sample 1A has a very large negative
magnetoresistance at low fields. This is interpreted
as a manifestation of the destruction, by the mag-
netic field, of bound magnetic polarons or magnetic
polarons, i.e., the magnetic field delocalized the
electrons which are magnetically trapped at zero
field. Above several kOe electrical conduction is
due to delocalized electrons in the conduction band.
In sample 4, many of the spin clusters apparently
overlap at zero field, so that the electrons can
move easily between the clusters. The zero-field
resistivity and low-field negative magnetoresistance
are therefore much smaller than in sample 1A.

C. High-field magnetoresistance

Figure 17 shows the high-field magnetoresistance
of sample 4 at 1.6 and 4.2 K. Similar data for sam-
ple 1A are shown in Fig. 18. In all cases ρ decreases
with increasing H_{ext}. The rate of change $|d\rho/dH_{ext}|$
also decreases with increasing H_{ext}, but is nonzero
even at the highest fields. Figure 19 shows the re-
sults for R_0 vs H_{ext} at 4.2 K, calculated from the
data of Fig. 8. Within the experimental uncertain-
ties R_0 is independent of H_{ext}. Analysis of these
results (including the experimental uncertainties)
shows that the negative magnetoresistance in sample
4 for $H_{ext} \geq 10$ kOe, and in sample 1A for $H_{ext} \geq 27$
kOe, is principally due to a change in μ and not to
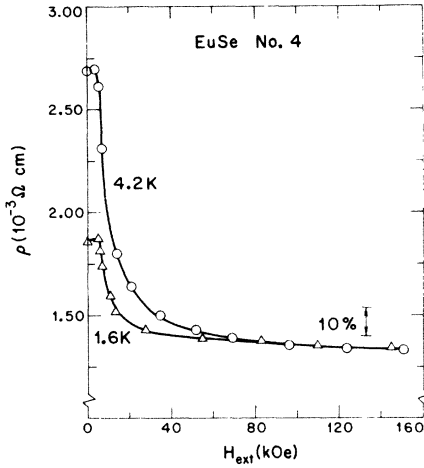a change in n. Note, however, that the Hall data

FIG. 17. Resistivity of sample 4 vs H_{ext} at 1.6 and 4.2 K. The magnitude of a 10% change in the high-field resistivity is indicated.

for sample 1A do not extend to magnetic fields below several kOe where magnetic trapping of electrons is presumed to occur.

The high-field negative magnetoresistance in Figs. 17 and 18 is interpreted as the result of a decrease in spin-disorder scattering with increasing H_{ext}. Spin-disorder scattering should disappear when the magnetization throughout the sample is saturated. The fact that in Figs. 17 and 18 the resistivity is still not completely independent of H_{ext} at 150 kOe suggests that the magnetization is still not completely saturated even at this field. Magnetization measurements show that at 4.2 K magnetic saturation is not achieved below 80 kOe (see Sec. III
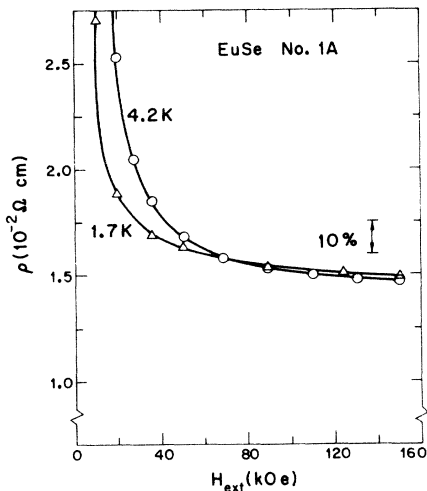

FIG. 18. Resistivity of sample 1A vs H_{ext} at 1.7 and 4.2 K. The very high resistivity at low fields is not shown (see Fig. 16). The magnitude of a 10% change in the high-field resistivity is indicated.
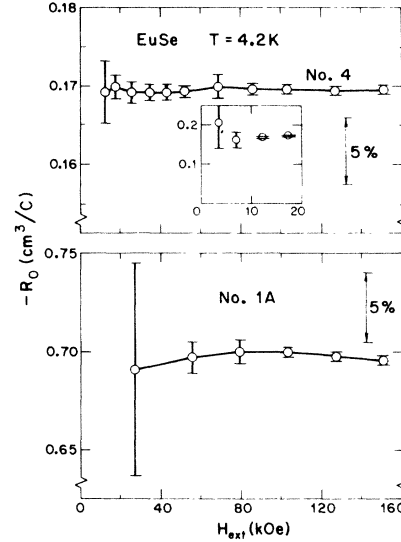

FIG. 19. R_0 vs H_{ext} for samples 4 and 1A at 4.2 K. (For corresponding resistivity data see Figs. 17 and 18.) Note that the ordinate scales are broken. The magnitude of a 5% change in R_0 is indicated. Low-field results for R_0 vs H_{ext} are shown in the insert for sample 4.

and Fig. 3). Changes of less than 1% in M between 100 and 150 kOe are not inconsistent with the magnetization data in Fig. 3.

XI. SUMMARY

The electrical transport properties of our EuSe samples are interpreted in terms of three physical processes:

a. Spin-disorder scattering. At temperatures well above T_{max} the electrical conductivity is due to electrons in the conduction band. The effects of the s-f (or d-f) interaction on ρ are described in terms of spin-disorder scattering which lowers the mobility. The application of a magnetic field reduces this scattering, leading to a negative magnetoresistance. The same description also applies for $T \lesssim T_{max}$ provided that H_{ext} is above ~ 10 kOe.

b. Electron trapping. When T is comparable to or lower than T_{max} and, in addition, $H_{ext} < 1$ to 10 kOe, the resistivity is very high (except for sample No. 4). This high resistivity is attributed to the localization (trapping) of the electrons due to s-f interaction. The application of a magnetic field $H_{ext} \gtrsim 10$ kOe results in the delocalization of the electrons, leading to band conduction and a much lower resistivity.

c. Spin splitting of the conduction band. A positive magnetoresistance occurs in a limited temperature range in fields below ~10^4 Oe. A model for this phenomenon is presented in the following paper.[16] In this model the spin splitting of the conduction band can lead to an increase in the scattering

of electrons by either ionized impurities or phonons. The resulting positive magnetoresistance can more than offset the negative magnetoresistance due to a decrease in spin-disorder scattering.

ACKNOWLEDGMENTS

*Visiting scientist at the Francis Bitter National Magnet Laboratory, Massachusetts Institute of Technology, Cambridge, Mass. 92139, on leave from University of São Paulo, Brazil, C. P. 8105.

†Supported by the National Science Foundation.

‡Work sponsored by the Department of the Air Force.

[1] S. Methfessel and D. C. Mattis, in *Handbuch der Physik*, edited by S. Flügge (Springer-Verlag, Berlin, 1968), Vol. 18, Pt. I.

[2] C. Haas, CRC Crit. Rev. Solid State Sci. 1, 47 (1970).

[3] Y. Shapira, S. Foner, and T. B. Reed, Phys. Rev. B 8, 2299 (1973); Y. Shapira, S. Foner, R. L. Aggarwal, and T. B. Reed, Phys. Rev. B 8, 2316 (1973).

[4] Y. Shapira, in *Proceedings of the International Conference on Magnetism, Moscow*, 1973 (Nauka, Moscow, to be published).

[5] Y. Shapira and T. B. Reed, Phys. Rev. B 5, 4877 (1972).

[6] Y. Shapira, S. Foner, N. F. Oliveira, Jr., and T. B. Reed, Phys. Rev. B 5, 2647 (1972).

[7] F. Holtzberg, T. R. McGuire, S. Methfessel, and J. C. Suits, in *Proceedings of the International Conference on Magnetism, Nottingham*, 1964 (The Institute of Physics and the Physical Society, London, 1964), p. 470.

[8] S. Methfessel, Z. Angew. Phys. 18, 414 (1965).

[9] S. von Molnar and S. Methfessel, J. Appl. Phys. 38, 959 (1967).

[10] S. von Molnar, IBM J. Res. Dev. 14, 269 (1970).

[11] S. von Molnar and T. Kasuya, in *Proceedings of the Tenth International Conference on the Physics of Semiconductors, Cambridge, Mass.*, 1970 (U. S. Atomic Energy Commission, Oak Ridge, Tenn., 1970), p. 233.

[12] A. Yanase and T. Kasuya, J. Phys. Soc. Jpn. 25, 1025 (1968).

[13] T. Kasuya and A. Yanase, Rev. Mod. Phys. 40, 684 (1968).

[14] A. Yanase and T. Kasuya, J. Appl. Phys. 39, 430 (1968).

[15] T. Kasuya, CRC Crit. Rev. Solid State Sci. 3, 131 (1972).

[16] Y. Shapira and R. L. Kautz, following paper, Phys. Rev. B 10, 4781 (1974).

[17] T. B. Reed and R. E. Fahey, J. Cryst. Growth 8, 337 (1971).

[18] F. Holtzberg, T. R. McGuire, S. Methfessel, and J. C. Suits, Phys. Rev. Lett. 13, 18 (1964).

[19] R. Griessen, M. Landolt, and H. R. Ott, Solid State Commun. 9, 2219 (1971).

[20] P. Schwob, Phys. Kondens. Mater. 10, 186 (1969).

[21] G. Petrich and T. Kasuya, Solid State Commun. 8, 1625 (1970).

[22] C. Kuznia and G. Kneer, Phys. Lett. A 27, 664 (1968).

[23] G. E. Everett and R. C. Jones, Phys. Rev. B 4, 1561 (1971).

[24] T. M. Kwon and G. E. Everett, in *Proceedings of the International Conference on Magnetism, Moscow*, 1973 (Nauka, Moscow, 1974), Vol. III, p. 520.

[25] T. Janssen, Phys. Kondens. Mater. 15, 142 (1972).

[26] T. Komaru, T. Hihara, and Y. Kōi, J. Phys. Soc. Jap. 31, 1391 (1971).

[27] P. G. de Gennes, Phys. Rev. 118, 141 (1960).

[28] E. L. Nagaev, Fiz. Tverd. Tela 11, 3438 (1969) [Sov. Phys.-Solid State 11, 2886 (1970)].

[29] E. L. Nagaev, Zh. Eksp. Teor. Fiz. 54, 228 (1968) [Sov. Phys.-JETP 27, 122 (1968)],

[30] T. Kasuya, in *Proceedings of the Tenth International Conference on the Physics of Semiconductors, Cambridge, Mass.*, 1970 (U. S. Atomic Energy Commission, Oak Ridge, Tenn., 1970), p. 243.

[31] J. B. Torrance, M. W. Shafer, and T. R. McGuire, Phys. Rev. Lett. 29, 1168 (1972).

[32] T. Kasuya, A. Yanase, and T. Takeda, Solid State Commun. 8, 1543 (1970).

[33] E. L. Nagaev, Zh. Eksp. Teor. Fiz. Pis'ma Red. 6, 484 (1967) [Sov. Phys.-JETP Lett. 6, 18 (1967)].

[34] M. Umehara and T. Kasuya, J. Phys. Soc. Jpn. 33, 602 (1972).

[35] J. Vitins and P. Wachter, in *Proceedings of the International Conference on Magnetism, Moscow*, 1973 (Nauka, Moscow, to be published).

[36] S. von Molnar and T. Kasuya, Phys. Rev. Lett. 21, 1757 (1968).

[37] W. A. Thompson, T. Penney, S. Kirkpatrick, and F. Holtzberg, Phys. Rev. Lett. 29, 779 (1972).

[38] T. Kasuya, Prog. Theor. Phys. 16, 58 (1956).

[39] R. A. Smith, *Semiconductors* (Cambridge U. P., Cambridge, England, 1959), Chap. 5.

[40] J. B. Torrance and F. Holtzberg, AIP Conf. Proc. 18, 902 (1974).

[41] In our view the resistivity peak in EuS is a separate phenomenon from the insulator-to-metal transition observed in this material (see Ref. 4).

[42] A. P. Grigin and E. L. Nagaev, Zh. Eksp. Teor. Fiz. Pis'ma Red. 16, 438 (1972) [Sov. Phys.-JETP Lett. 16, 312 (1972)].